X-linked hypomyelination with spondylometaphyseal dysplasia (H-SMD) associated with mutations in AIFM1

Miyake, Noriko; Wolf, Nicole I.; Cayami, Ferdy K.; Crawford, Joanna; Bley, Annette; Bulas, Dorothy; Conant, Alex; Bent, Stephen J.; Gripp, Karen W.; Hahn, Andreas

Published in:
Neurogenetics

DOI:
10.1007/s10048-017-0520-x

Publication date:
2017

D. Brief Conclusion

Stealth and anti-radar missiles will become threats to military radar, but the techniques countering them will also advance. The common effective measures to counter the two threats are the use of bistatic and multistatic systems and lower carrier frequency. Some techniques in common with ECCM, such as low probability of interception techniques (include ultra-low-sidelobe antenna, frequency agility, flexible coded signal, etc.), bistatic and multistatic, weak signal detection and the capability of radar flexibility. Obviously, at the present, these techniques should be the focal point of radar technique research.

LI NENG-JING
Chinese Institute of Electronics
P.O. Box 2862
Beijing 10085
People's Republic of China

REFERENCES

[1] Neng-jing, L., et al. (1985)
On radar jamming and radar counter jamming, acta.
Electronica SIMCA, **12**, 1 (1985), 99.

[2] Peikong, H. (1984)
A discussion of aircraft stealth technology.
Systems Engineering and Electronic Technology, **1** (1984), 1–8.

[3] Boyle, D. (1982)
Anti-radar missile.
Interavia Aerospace Review, **1** (1982), 1194–1195.

[4] Chaopei, L. (1985)
Anti-radiation missiles and their guidance technology.
Cruise Missiles, **4** (1985), 25–32.

[5] Barbow, J., et al. (1984)
An ARM simulation model.
Military microwave (1984), London, 544–547.

[6] Moraitis, D., et al. (1985)
Effect of radar frequency on the detection shaped targets.
IEEE Radar-85, 159–162.

[7] Bachman, C. G. (1982)
Radar Targets.
Lexington Books, 1982.

[8] Jacques, D., et al. (1984)
Une approche nouvellë du radar de surveillance aërienne.
ICR-84, Paris, 505–520.

[9] Westinghouse (1985)
Surveillance radar, a brochure of Westinghouse command and control division.
Westinghouse, 1985.

[10] Farina, A., and Galati, G. (1985)
An overview of current and advanced signal processing techniques for surveillance radar.
IEEE Radar-85, 175–183.

[11] Nelson, G. R., et al. (1982)
HF sky-wave radar for over-the-horizon detection.
IEE Radar-82, 244–247.

[12] Chrispin, J. W., Jr., et al. (1968)
Methods of Radar Cross-Section Analysis.
New York: Academic Press, 1968.

[13] Fleming, P. L., and Wills, N. J. (1980)
Sanctuary radar.
Proceedings of 2nd Military microwave Conference.
London, (1980), 103–108.

[14] Lee, P. K. (1985)
Space based bistatic radar: Opportunity for future tactical air surveillance.
IEEE Radar-85, 322–329.

[15] Marshell, J., et al. (1982)
A barrier radar concept.
IEE Radar-82, 115–119.

[16] Hussain, M. G. M. (1985)
An overview of developments in nonsinusoidal wave technology.
IEEE Radar-85, 184–189.

[17] Giuli, D., et al. (1982)
Performance evaluation of some adaptive polarization techniques.
IEE Radar-82, 76–81.

[18] Hong, J. Y., et al. (1983)
Detection of weak 3rd harmonic backscatter from nonlinear metal targets.
EASCON Record (July 1983), 169.

[19] Wiley, R. G. (1985)
Electronic Intelligence, the Interception of Radar Signals.
Dedham, MA: Artech House, 1985.

[20] O'Reilly, G. T., et al. (1982)
Track-while-scan quiet radar.
IEEE 1982 EASCON.

[21] Barton, M. (1981)
Adaptive radar sharpens NATO's defense.
Microwaves, **20**, 4 (Sept. 1981), 19–22.

[22] Parker, C. H. (1983)
The design and performance of modern 2-D medium range defense radars.
In *Proceedings of International Radar Symposium in India*, (1983), 430-435.

[23] van Brunt, L. B. (1978)
Applied ECM.
EW Engineering Inc., 1978.

[24] Astia Document 007859.
A netted search radar system.

[25] Spaulding, W. G. (1981)
A dispersed radar concept for air defense.
Astia Document A122256, July 1981.

[26] (1984)
Long range air defense radar increases anti-radiation missile capability.
Modern Radar Trends, **5** (1984), 22.

Multitarget Detection Using Synthetic Sampled Aperture Radars

A new multitarget detection technique using synthetic sampled aperture radar (SSAMAR) is presented. In contrast with the standard approach to multitarget detection, this technique may not require the use of phase shifting or tapering hardware. SSAMAR doubles the target pattern resolution, attenuates the sidelobes to about −27 dB, and significantly enhances the signal-to-noise ratio (SNR). Computer simulation is used to illustrate and validate this technique. Multitarget patterns for both standard and SSAMAR operations are provided.

Manuscript received June 5, 1992; revised January 11, 1994.

IEEE Log No. T-AES/31/3/12734.

I. INTRODUCTION

The standard approach to multitarget detection is to use phased array radars with tapering and phase shifting hardware. The array elements are excited in parallel to form a beam of width (λ/Nd), where λ is the wavelength, N is the number of sensors, and d is the element spacing. The synthesis of L simultaneous beams requires the use of L sets of phase shifters operating in the steady state [1, 2].

In principle, multitarget detection is equivalent to synthesizing multiple beams (beamforming) with independent controls. This requires emphasizing the return signals in certain directions while attenuating the interference in other directions. Multiple beams can be formed at the transmitting or receiving modes. Also, it can be carried out at the RF, IF, baseband, or digital levels. RF beamforming is the simplest and most common technique. In this case, multiple narrow beams are formed through the use of phase shifters. IF and baseband beamforming require complex coherent hardware. However, the system is operated at lower frequencies where tolerance is not as critical. Digital beamforming is more flexible than RF, IF, or baseband techniques, but it requires a demanding level of parallel very large-scale integrated (VLSI) processing hardware [1].

This correspondence presents a new multitarget detection technique based on discrete processing of synthetic sampled aperture radar (SSAMAR) signals. In this approach, the array elements are fired sequentially, one at a time, while all elements receive in parallel. The returned sgnals at each sensor are integrated coherently to synthesize a complex information vector. This effectively synthesizes a two-way multiple beam pattern without the need for phase shifting or tapering hardware [3–6]. The field of view is defined by the 3 dB beamwidth of one sensor. All targets within this field of view will simultaneously reflect the incident electric field. It follows that the returned field sensed by the array is made of all spatial frequencies corresponding to the targets angular locations. Therefore, the task of multitarget detection is transformed into a spectral estimation problem. Conventional spectrum estimation techniques can then be used in the signal processing. Spectral peaks will correspond to angular locations of the targets. The new technique is valid for fixed and synthetic arrays.

II. CONVENTIAL BEAMFORMING

Consider a linear array of N equally spaced elements, and a plane wave incident on the aperture with direction-sine $\sin\beta$, as shown in Fig. 1. Conventional beamformers appropriately delay the outputs of each sensor to form a beam steered at angle

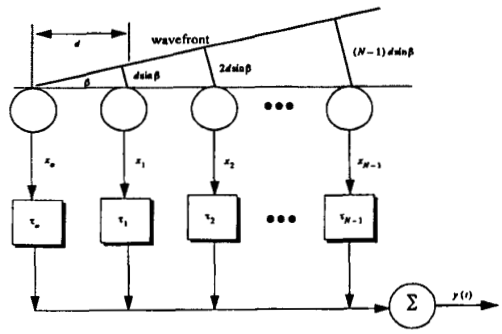

Fig. 1. Linear array of size N, element spacing d, incident plane wave defined by $\sin\beta$.

β. The output of the beamformer is,

$$y(t) = \sum_{n=0}^{N-1} x_n(t - \tau_n) \tag{1}$$

$$\tau_n = (N - 1 - n)\frac{d}{c}\sin\beta; \qquad n = 0, N-1 \tag{2}$$

where d is the element spacing, and c is the speed of light. Fourier transformation of (1) yields,

$$Y(\omega) = \sum_{n=0}^{N-1} X_n(\omega)\exp(-j\omega\tau_n) \tag{3}$$

which can be written in vector form as

$$\vec{Y} = \vec{a}^{\dagger}\vec{X} \tag{4}$$

$$\vec{a}^{\dagger} = [\exp(j\omega\tau_0)\exp(j\omega\tau_1)\cdots\exp(j\omega\tau_{N-1})] \tag{5}$$

$$\vec{X}^{\dagger} = [X_0(\omega)\ X_1(\omega)\cdots X_{N-1}(\omega)]^{*} \tag{6}$$

where the superscript † indicates complex conjugate transpose.

Let A_1 be the amplitude of the wavefront defined by $\sin\beta_1$, then the vector $\vec{X}$ is

$$\vec{X} = A_1\vec{s}_{k1}^{*} \tag{7}$$

where $\vec{s}_{k1}$ is a steering vector, and in general $\vec{s}_k$ is given by

$$\vec{s}_k^{\dagger} = [1 \cdot \exp(-jk) \cdot \cdots \cdot \exp(-j(N-1)k)]$$
$$k = \frac{2\pi d}{\lambda} \cdot \sin\beta. \tag{8}$$

Ignoring the phase term $\exp(-j(N-1)k)$, we can write (5) as

$$\vec{a} = \vec{s}_k \tag{9}$$

and the beamformer output will be

$$\vec{Y} = \vec{a}^{\dagger}\vec{X} = A_1\vec{s}_{k1}^{\dagger}\vec{s}_k. \tag{10}$$

The array pattern of the beam steered at k_1 is computed as the expected value of $\vec{Y}$. In other words,

$$S(k) = E\{\vec{Y}\vec{Y}^{\dagger}\} = P_1\vec{s}_k^{\dagger}\Re\vec{s}_k \tag{11}$$

where $P_1 = E\{|A_1|^2\}$ and $\Re$ is the correlation matrix. If $\vec{X} = A_1\vec{s}^*_{k1}$, then the power spectrum is

$$S(k) = P_1\vec{s}^{\dagger}_k\vec{s}_{k1}\vec{s}^{\dagger}_{k1}\vec{s}_k. \tag{12}$$

Consider L incident plane waves with directions of arrival defined by

$$k_i = \frac{2\pi d}{\lambda}\sin\beta_i; \qquad i = 1, L. \tag{13}$$

The nth sample at the output of the mth sensor is

$$y_m(n) = v(n) + \sum_{i=1}^{L} A_i(n)\exp(-jmk_i); \qquad m = 0, N-1 \tag{14}$$

where $A_i(n)$ is the amplitude of the ith plane wave, and $v(n)$ is white, zero-mean noise with variance σ_v^2, and it is assumed to be uncorrelated with the signals. Equation (14) can be written in vector notation as,

$$\vec{y}(n) = \vec{v}(n) + \sum_{i=1}^{L} A_i(n)\vec{s}^*_{ki}. \tag{15}$$

A set of L steering vectors is needed to simultaneously form L beams. Define the steering matrix $\mathcal{X}$ as

$$\mathcal{X} = [\vec{s}_{k1}\ \vec{s}_{k2}\cdots\vec{s}_{kL}]. \tag{16}$$

Then the autocorrelation matrix of the field measured by the array is

$$\Re = E\{\vec{y}(n)\vec{y}^{\dagger}(n)\} = \sigma_v^2\mathbf{I} + \mathcal{X}\mathbf{C}\mathcal{X}^{\dagger} \tag{17}$$

where $\mathbf{C} = \text{diag}[P_1\ P_2\cdots P_L]$, and $\mathbf{I}$ is the identity matrix.

The array pattern can now be computed using standard spectral estimators. For example, using the Bartlett beamformer, yields

$$\widehat{S}(k) = \vec{s}^{\dagger}_k\Re\vec{s}_k. \tag{18}$$

The spectrum defined by (18) generates spectral peaks at angles β_i for each wavefront defined by k_i. Assuming the ith wavefront, then the signal-to-noise ratio (SNR) is [7]

$$\text{SNR} = N\left(\frac{P_i}{\sigma_v^2}\right). \tag{19}$$

III. SYNTHETIC SAMPLED APERTURE RADAR

The strength of sampled aperture radar (SAMAR) comes from its receiver, and its distinct signal processing techniques [8]. SSAMAR can be achieved through sequential firing of the array elements. In this case, an array twice as large as the actual one is synthesized. It follows that the angular resolution is doubled compared with the standard operation and the SNR is greatly improved. Sequential mode operation

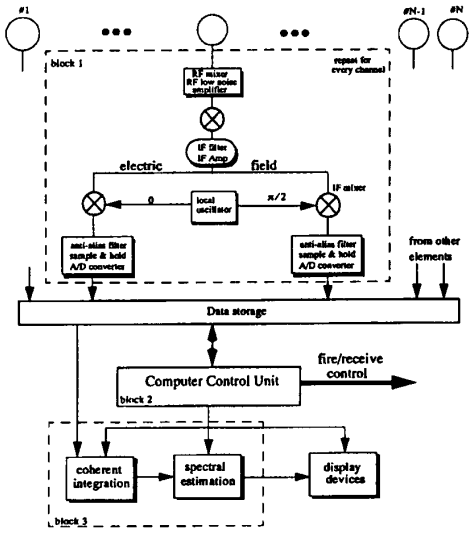

Fig. 2. Block diagram for SSAMAR receiver.

was first introduced in [9–12], where the authors' main interest was focused on Matrix Hologram Radar development. A typical SSAMAR receiver is shown as part of Fig. 2, which consists of three main blocks: 1) sampled aperture antenna, 2) computer control unit, and 3) a signal processing block.

A. Operation

Consider the array shown in Fig. 2. SSAMAR operation can be described as follows. The firing of the elements is sequential, one at a time, while all elements receive in parallel. The echo signals are collected and stored coherently on the basis of equal two-way geometric phase. A complex information sequence $\{b(m);\ m = 0, 2N-2\}$ is synthesized. The two-way array pattern is computed as the amplitude spectrum of $\{b(m)\}$. The synthesized sequence has natural triangular windowing, and the sidelobes are about -27 dB, thus extra tapering may not be required [3, 4].

The information sequence is generated from the N^2 returns, and is computed as follows

$$m = i + j; \qquad (i, j) = 0, N-1 \tag{20}$$

$$b(m) = p(i, j)\exp(j\phi_i)\exp(j\phi_j) \tag{21}$$

$$\phi_i = \left(-\left(\frac{N-1}{2}\right) + i\right)\Delta\phi \tag{22}$$

$$\phi_j = \left(-\left(\frac{N-1}{2}\right) + j\right)\Delta\phi \tag{23}$$

$$\Delta\phi = \frac{2\pi d}{\lambda}\sin\beta \tag{24}$$

where $p(i,j) = 1$ if the path, ith element transmitting and jth element receiving exists, otherwise it is equal to zero, and $\sin\beta$ is the direction-sine towards which the radiation pattern is steered. The information sequence has $N_a = 2N - 1$ distinct entries.

The components of the information sequence has linear phase, and the phase increment between any two adjacent terms is equal to $\Delta\phi$. The sequence $\{b(m)\}$ also has triangular shape weighting, defined by

$$\{c(m);\ m = 0,2N-2\} = \left\{ \begin{array}{ll} m+1; & m = 0,N-2 \\ N; & m = N-1 \\ 2N-1-m; & m = N,2N-2 \end{array} \right\}. \quad (25)$$

Through zero padding, the sequence $\{b(m)\}$ is extended to the next power of 2. The two-way pattern in the direction $\sin\beta$, is computed as the modulus of the discrete Fourier transform (DFT) of the extended sequence $\{b(m)\}$.

Assume an incident plane wave defined by amplitude A_1 and direction-sine $\sin\beta_1$, and zero-mean, white additive noise v with variance σ_v^2. Then, the mth sample of the information sequence is

$$b(m) = A_1 s(m) + v(m); \qquad m = 0, N_a - 1 \quad (26)$$

$$A_1 = G_e^2(\sin\beta_1)\left(\frac{R_0}{R}\right)^4 \rho_1 \quad (27)$$

$$s(m) = c(m)\exp\{j[m-(N-1)]k_1\} \quad (28)$$

where G_e^2 represents the two-way element gain, R_0 is the reference range, and ρ_1 is the wave amplitude. It follows that if there are L incident plane waves dfined by $\{\sin\beta_i;\ i = 1,L\}$, then the composite information sequence is

$$b(m) = \sum_{i=1}^{L} A_i s_i(m) + v(m); \qquad m = 0, \quad N_a - 1 \quad (29)$$

which can be written in vector notation as

$$\vec{b} = \sum_{i=1}^{L} A_i \vec{s}_i + \vec{v}. \quad (30)$$

B. Electronic Processing

Assuming that the noise is spatially incoherent and is uncorrelated with the signal samples, then the autocorrelation matrix for the field sensed by the array is

$$\Re = E\{\vec{b}\vec{b}^{\dagger}\} = \sigma_v^2 I + \sum_{i=1}^{L} P_i \vec{s}\vec{s}^{\dagger}. \quad (31)$$

Discrete Fourier transformation of the sequence $\{b(m)\}$ yields,

$$B(q) = \sum_{m=0}^{N_a-1} b(m)\exp\left(-j\frac{2\pi qm}{N_a}\right); \qquad q = 0, N_a - 1 \quad (32)$$

which can be expressed as the dot product

$$B(q) = \vec{a}^{\dagger}(q)\cdot\vec{b} \quad (33)$$

where

$$a(q;m) = \exp\left(j\frac{2\pi qm}{N_a}\right). \quad (34)$$

The power at the output of the signal processor at frequency bin q is

$$p(q) = E\{|B(q)|^2\} = E\{(\vec{a}^{\dagger}(q)\vec{b})(\vec{a}^{\dagger}(q)\vec{b})^{\dagger}\} = \vec{a}^{\dagger}(q)\Re\vec{a}(q) \quad (35)$$

where $\Re$ is defined in (31). Thus,

$$P(q) = \sigma_v^2\vec{a}^{\dagger}(q)I\vec{a}(q) + \sum_{i=1}^{L} P_1\vec{a}^{\dagger}(q)\vec{s}_i\vec{s}_i^{\dagger}\vec{a}(q). \quad (36)$$

After compensation for range attenuation and antenna gain, spectral peaks will be proportional to amplitudes of incident waves. For example, a peak at an arbitrary bin q_j will correspond to a plane wave defined by direction-sine $\sin\beta_j$. It follows that

$$P(q_j) = 2N\sigma_v^2 + N^4 P_j + \sum_{\substack{i=1 \\ i\neq j}}^{L} P_i\vec{a}^{\dagger}(q_j)\vec{s}_i\vec{s}_i^{\dagger}\vec{a}(q_j). \quad (37)$$

The first term of the right-hand side of (37) represents the noise power at q_j. The last term corresponds to spectral leakage, while the signal power at q_j is given by the middle term. Note that the sequence $\{c(m)\}$ is the reason for the N^4 factor. More precisely,

$$N^4 = \sum_{m=0}^{2N-2}[c(m)]^2. \quad (38)$$

Thus, the SNR is

$$\mathrm{SNR}|_{q_j} = \left(\frac{N^3}{2}\right)\left(\frac{P_j}{\sigma_v^2}\right). \quad (39)$$

Examination of (19) and (39) indicates that the SNR improvement factor using SSAMAR operation and signal processing, assuming equal transmitted power, is

$$I_{\mathrm{SNR}} = (20\log N - 6)\ \mathrm{dB}. \quad (40)$$

However, since in most practical systems a single element gain is less than that for a whole array, the

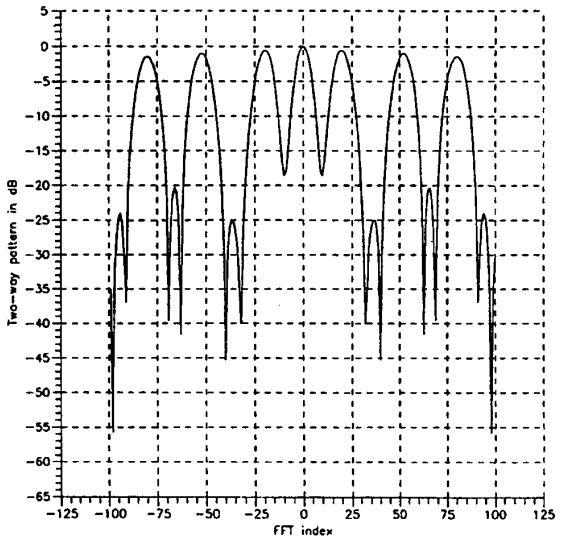

Fig. 3. Multitarget two-way pattern using standard processing.

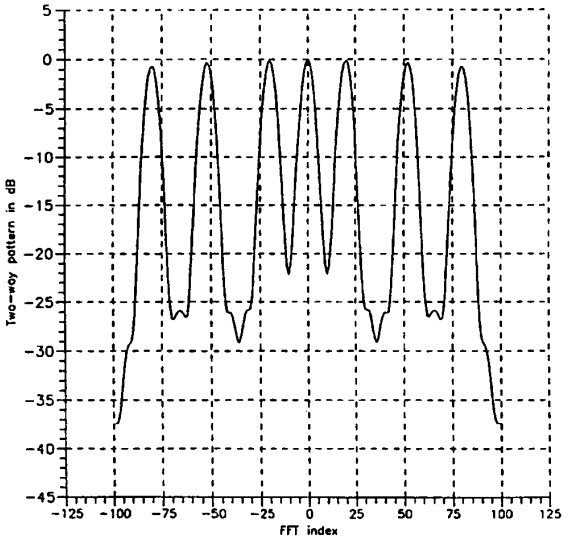

Fig. 4. Multitarget two-way pattern using SSAMAR processing.

SNR improvement factor may be lower than that given in (40).

IV. EXAMPLES

The two examples presented assume the following: 1) array field of view spans $-1.79°$ to $1.79°$; 2) circular sensors of diameter $D = 16\lambda$; 3) detection of seven unit scatterers at angular locations $\{\beta_i;\ i = 1,7\} = \{-1.119°, -0.783°, -0.279°, 0.0°, 0.279°, 0.783°, 1.119°\}$; 4) a linear array of size $N = 64$; 5) both examples assume a Kaiser window with parameter equal to π. Example 1 demonstrates detection using the standard approach as described in Section II. Fig. 3 shows the multitarget pattern corresponding to this case. In Example 2, SSAMAR multitarget detection is demonstrated. In this case, no phase shifting hardware is required. Fig. 4 shows the synthesized target pattern for this case. Frequency interpolation has been used in both examples for better display of the results.

Observation of Figs. 3 and 4 indicates that all targets have been detected at the proper locations. However, SSAMAR multitarget detection synthesizes a pattern which is twice as narrow compared with the standard case. Also, the sidelobe levels for SSAMAR case are lower than the standard case.

V. CONCLUSIONS

A new approach for multitarget detection, using SSAMAR processing techniques was presented. In this case, the return signals are collected and integrated coherently on the basis of equal two-way geometric phase. A complex information vector is synthesized. No phase shifting or tapering hardware is required. SSAMAR significantly improves the SNR. The array field of view is defined by the 3 dB beamwidth of one element. It follows that the returned field sensed by the array is made of all spatial frequencies corresponding to the angular locations of the targets. Therefore, the task of multitarget detection is transformed into a spectral estimation problem. Spectral peaks will correspond to angular locations of the targets.

Examples through computer simulation demonstrated multitarget detection using both standard and SSAMAR techniques. The SSAMAR approach has several advantages over the standard approach: 1) multitarget detection is performed without phase shifting hardware; 2) the SNR is significantly improved; and 3) the approach is quite general and can be applied to synthetic or real arrays.

BASSEM R. MAHAFZA
KBM Enterprises, Inc.
15980 Chaney Thompson Rd.
Huntsville, AL 35803

LEE H. HEIFNER
VINCENT C. GRACCHI
Dynetics, Inc.
P.O. Box Drawer B
Huntsville, AL 35814

REFERENCES

[1] Scanlan, M. (Ed.) (1987)
Modern Radar Techniques.
New York: Macmillan, 1987.

[2] Skolnik, M. (Ed.) (1990)
Radar Handbook (2nd ed.).
New York: McGraw-Hill, 1990.

[3] Mahafza, B. (1989)
Two and three-dimensional synthetic aperture radar imaging using a linear array with transverse motion.
Ph.D. dissertation, University of Alabama at Huntsville, Mar. 1989.

[4] Mahafza, B., and Polge, R. (1990)
Multiple target detection through DFT processing is a sequential mode operation of real two-dimensional arrays.
In *IEEE SoutheastCon '90*, New Orleans, LA, Apr. 1990, 167–170.

[5] Polge, R., Mahafza, B., and Kim, J. (1989)
Focusing linear arrays operating in a sequential mode.
In *IEEE SoutheastCon '89*, Columbia, SC, Apr. 1989, 171–174.

[6] Rhea, J., Mahafza, B., and Audeh, N. (1993)
Radar interference cancellation using sequential mode operation (ICSEQ).
Journal of the Franklin Institute, **330**, 2 (Mar. 1993), 413–421.

[7] Orfanidis, S. (1988)
Optimum Signal Processing: An Introduction (2nd ed.).
New York: McGraw-Hill, 1988.

[8] Lo, T., and Litava, J. (1991)
Low angle tracking using a multifrequency sampled aperture radar.
IEEE Transactions on Aerospace and Electronic Systems, **7**, 5 (Sept. 1991), 797–805.

[9] Ogura, H., and Fukouka, S. (1976)
Imaging of a two-dimensional target by means of hologram matrix.
Proceedings of the IEEE (Mar. 1976), 364–365.

[10] Izuka, K., Ogura, H., Yen, J., Nguyen, V., and Weedmark, J. (1976)
A hologram matrix radar.
Proceedings of the IEEE (Oct. 1976), 1493–1504.

[11] Nakayama, J., Miyashita, T., Akagai, N., Ogura, H., Yoshida, Y., and Soma, T. (1978)
Imaging of a two-dimensional target by means of hologram matrix—An ultrasound experiment.
Proceedings of the IEEE (Oct. 1978), 1287–1290.

[12] Nakayama, J., Ogura, H., Miyashita, T., and Shibayama, T. (1979)
Two-dimensional imaging of multifrequency hologram matrix—An ultrasound experiment.
Proceedings of the IEEE (Dec. 1979), 1669–1771.

A Necessary Condition for Effective Performance of the Multiple Model Adaptive Estimator

Effective adaptive estimation for a general linear system driven by an input modeled by a randomly switching Gaussian process is considered. The performance of the multiple model adaptive estimator (MMAE) is, in some cases, unexpectedly hampered by a necessary condition not satisfied by the linear system. This key dependency for effective MMAE performance is based on a particular property of the DC gain of the linear system.

Manuscript received November 12, 1993; revised June 10, 1994.

IEEE Log No. T-AES/31/3/12735.

This work was supported by the Office of Naval Research under Grant N00014-89-J-3123.

I. INTRODUCTION

The use of adaptive estimation algorithms involving Kalman filters has been a topic of great interest for many years. The need for adaptive algorithms surfaced as typical estimation applications became more complex. Brown [1] states that in a typical application the various parameters that describe the system model are assumed to be known. Even if they are time-varying, the variation is assumed to be known. The parameters are then used in the Kalman filter design to reflect the knowledge of the system model. For more complex and practical problems, the parameters may not be known exactly or may change at unknown times. In such cases, it is highly desirable to design the filter to be self-learning, so that it can adapt itself to the particular situation at hand.

The pioneering work in this area was formulated by Magill [2]. He considered the problem of estimation of a Gaussian random process when a parameter vector of the process is initially unknown and remains constant with time. The actual parameter vector is assumed to come from a set of N a priori known vectors. A bank of N Kalman filters, operating in parallel, is formed, with each filter based on a unique parameter vector from the known set. The individual filter outputs are appropriately weighted and then summed to produce the overall optimal estimate. The weighting coefficients are determined by a nonlinear function of the measurement residuals of the individual filters. The correct filter is that individual filter based on the parameter vector equal to the actual parameter vector of the Gaussian random process. The weighting coefficient value of the correct filter will tend toward one, while the weighting coefficient values of the remaining mismatched model filters will tend toward zero.

This basic adaptive estimation technique is described in the literature under various names such as the self-learning algorithm [1], the parallel processing algorithm [3], the modified Gaussian sum adaptive filter [4, 5], the multiple model estimation algorithm [6], and the multiple model adaptive estimator (MMAE) [7]. The MMAE has been extended to handle a variety of new situations and applications. Ackerson and Fu [8] developed an adaptive state estimator for a linear system operating in a switching environment, with transitions from one Gaussian noise source to the next governed by a Markov transition probability matrix. Moose and Wang [9] modeled the variations in a switching plant by a semi-Markov process. A semi-Markov process is a Markov process whose transition times can also be arbitrary random variables [10]. Caputi and Moose [11] modified the Gaussian sum adaptive filter of [12] using a semi-Markov switching process to handle non-Gaussian inputs. All these and others [13–15] have used the MMAE with good success.